Periodica Polytechnica Civil Engineering, 70(1), pp. 175–188, 2026

An Automated Bipartite Graph-based Force Method for Efficient Analysis of Planar Trusses

Ali Kaveh[1*], Seyed Abdolrahman Hosseini[1]

[1] School of Civil Engineering, Iran University of Science and Technology, P. O. B. 16765-163, Narmak, 16846-13114 Tehran, Iran
[*] Corresponding author, e-mail: alikaveh@iust.ac.ir

Received: 24 December 2025, Accepted: 06 February 2026, Published online: 16 February 2026

Abstract

Efficient analysis of structures refers to the methods which reduce the computational cost of the structural analysis. To achieve this, the structural matrices should have some specific attributes. For this purpose, a graph theoretical force method is employed in this study, which leads to a sparse flexibility matrices. In this method, the bipartite graph corresponding to the equivalent graph of the original structural model is constructed. A cycle basis of the bipartite graph corresponds to subgraphs of the structural model on which localized self-equilibrating stress systems can be formed, referred to as a generalized cycle basis of the structure. This enabled the authors of this study to develop a fully automated procedure for the efficient analysis of planar trusses using a graph-theoretical force method. The proposed approach combines classical structural mechanics with the concepts of graph theory. In other words, a bipartite graph approach is employed for a systematic identification of self-equilibrating stress systems in the truss structures. The entire procedure is implemented in MATLAB, allowing all steps to be performed automatically and three different planar trusses are solved using proposed method.

Keywords

force method, graph theory, planar truss, flexibility matrix, statical basis, self-equilibrating stress systems

1 Introduction

The force method is a classical technique in structural analysis in which the internal forces of the members are treated as the primary unknowns, while the displacement method determines the nodal displacements first and then computes the corresponding internal forces.

Accordingly, when the force method is applied to a structure, which has a degree of static indeterminacy (DSI) less than the degree of kinematic indeterminacy (DKI), the resulting matrices are smaller in size than those obtained using the displacement method. This leads to faster computational performance, particularly in iterative methods which has been used for structural optimization of large-scale structures with numerous members. However, in the structures with smaller DKI, the displacement method can be more efficient.

Topological force method was developed by De C. Henderson [1] and De Henderson and Maunder [2] for rigid-jointed skeletal structures by a manual selection of the cycle bases for their graph models [3]. Methods suitable for computer are due to Kaveh [4–6]. Although, Kaveh [7] generalized the topological methods for various types of skeletal structures, such as pin-jointed planar trusses, ball-jointed space trusses and rigid-jointed frames.

Algebraic methods have also been developed and extended by Denke [8], Robinson and Haggenmacher [9], Topçu [10], Kaneko et al. [11], Soyer and Topcu [12] and Kaveh and Shabani Rad [13]. Mixed algebraic-topological methods are due to Gilbert and Heath [14], Coleman and Pothen [15, 16], and Pothen [17]. Simultaneous analysis and design can be found in the work of Kaveh and Rahami [18], and Kaveh and Bijari [19] among many others. These methods are simple, however the used techniques reveal limited information about the utilized concepts. In addition, Grubits et al. [20] and Grubits and Movahedi Rad [21] have investigated the optimal elasto-plastic design of truss structures using metaheuristic optimization algorithms.

Two graph theoretical approaches are introduced by Kaveh [22] to generate a statical basis yielding sparse flexibility matrices for planar truss structures. The first approach employs the associated graph, which was recently investigated by Kaveh [23] and Kaveh and Khavaninzadeh [24, 25]. The second approach employs a bipartite graph, which is used by the authors in this study to create a fully automated procedure for the efficient analysis of planar trusses using the force method in MATLAB [26]. It should be noted that all graphical illustrations presented in this study were also generated using MATLAB R2021a [26].

2 Force method for truss structures

For a structure S with M members and N nodes, which is $\gamma(S)$ times statically indeterminate, $\gamma(S)$ independent unknown forces should be selected as redundants. External reactions and/or internal forces of the structure can be chosen as redundants. These redundants are considered by

$$\boldsymbol{q} = \left\{\boldsymbol{q}_1, \boldsymbol{q}_2, \ldots, \boldsymbol{q}_{\gamma(S)}\right\}^{\mathrm{T}} . \tag{1}$$

Where the superscript T denotes the transpose operator.

The constraints corresponding to redundants are removed to obtain the corresponding statically determinate structure, known as the basic structure of S. It is important to note that a basic structure should be rigid. Denote the joint loads as

$$\boldsymbol{p} = \left\{\boldsymbol{p}_1, \boldsymbol{p}_2, \ldots, \boldsymbol{p}_n\right\}^{\mathrm{T}} . \tag{2}$$

Where n is equal to the number of components for applied point loads.

For a linear analysis conducted via the force method, the stress resultant distribution $\boldsymbol{r}$ corresponding to the applied load $\boldsymbol{p}$ may be represented as

$$\boldsymbol{r} = \boldsymbol{B}_0 \boldsymbol{p} + \boldsymbol{B}_1 \boldsymbol{q} . \tag{3}$$

Here, $\boldsymbol{B}_0$ and $\boldsymbol{B}_1$ are rectangular matrices, each with m rows and n and $\gamma(S)$ columns, respectively, where m represents the number of independent components of the member forces. $\boldsymbol{B}_0\boldsymbol{p}$ is referred to as the particular solution, which satisfies equilibrium under the applied load, while $\boldsymbol{B}_1\boldsymbol{q}$ denotes the complementary solution, constructed from a maximal set of independent self-equilibrating stress systems (SESs), commonly known as a statical basis. The force-displacement relationships are expressed as follows:

$$\boldsymbol{u} = \boldsymbol{F}_m \boldsymbol{r} = \boldsymbol{F}_m \boldsymbol{B}_0 \boldsymbol{p} + \boldsymbol{F}_m \boldsymbol{B}_1 \boldsymbol{q} . \tag{4}$$

In matrix form is

$$[\boldsymbol{u}] = [\boldsymbol{F}_m][\boldsymbol{B}_0 \quad \boldsymbol{B}_1]\begin{bmatrix} \boldsymbol{p} \\ \boldsymbol{q} \end{bmatrix}, \tag{5}$$

from the principle of virtual work:

$$[\boldsymbol{v}] = \begin{bmatrix} \boldsymbol{B}_0^{\mathrm{T}} \\ \boldsymbol{B}_1^{\mathrm{T}} \end{bmatrix}[\boldsymbol{u}] . \tag{6}$$

Combining Eq. (5) and Eq. (6), we have

$$\begin{bmatrix} \boldsymbol{v}_0 \\ \boldsymbol{v}_c \end{bmatrix} = \begin{bmatrix} \boldsymbol{B}_0^{\mathrm{T}} \\ \boldsymbol{B}_1^{\mathrm{T}} \end{bmatrix}[\boldsymbol{F}_m][\boldsymbol{B}_0 \quad \boldsymbol{B}_1]\begin{bmatrix} \boldsymbol{p} \\ \boldsymbol{q} \end{bmatrix} . \tag{7}$$

In which $\boldsymbol{v}_0$ represents the displacements associated with the force components of $\boldsymbol{p}$, and $\boldsymbol{v}_c$ indicates the relative displacements at the cuts of the basic structure. Carrying out the multiplication yields:

$$\begin{bmatrix} \boldsymbol{v}_0 \\ \boldsymbol{v}_c \end{bmatrix} = \begin{bmatrix} \boldsymbol{B}_0^{\mathrm{T}} \boldsymbol{F}_m \boldsymbol{B}_0 & \boldsymbol{B}_0^{\mathrm{T}} \boldsymbol{F}_m \boldsymbol{B}_1 \\ \boldsymbol{B}_1^{\mathrm{T}} \boldsymbol{F}_m \boldsymbol{B}_0 & \boldsymbol{B}_1^{\mathrm{T}} \boldsymbol{F}_m \boldsymbol{B}_1 \end{bmatrix}\begin{bmatrix} \boldsymbol{p} \\ \boldsymbol{q} \end{bmatrix} . \tag{8}$$

Defining

$$\begin{aligned} \boldsymbol{D}_{00} &= \boldsymbol{B}_0^{\mathrm{T}} \boldsymbol{F}_m \boldsymbol{B}_0 \\ \boldsymbol{D}_{01} &= \boldsymbol{B}_0^{\mathrm{T}} \boldsymbol{F}_m \boldsymbol{B}_1 \\ \boldsymbol{D}_{10} &= \boldsymbol{B}_1^{\mathrm{T}} \boldsymbol{F}_m \boldsymbol{B}_0 \\ \boldsymbol{D}_{11} &= \boldsymbol{B}_1^{\mathrm{T}} \boldsymbol{F}_m \boldsymbol{B}_1 , \end{aligned} \tag{9}$$

where the $\boldsymbol{D}_{11}$ is known as the flexibility matrix of structure.

We have

$$\boldsymbol{v}_0 = \boldsymbol{D}_{00} \boldsymbol{p} + \boldsymbol{D}_{01} \boldsymbol{q} \tag{10}$$

and

$$\boldsymbol{v}_c = \boldsymbol{D}_{10} \boldsymbol{p} + \boldsymbol{D}_{11} \boldsymbol{q} . \tag{11}$$

Considering the compatibility conditions as

$$\boldsymbol{v}_c = 0 , \tag{12}$$

combining Eq. (12) with Eq. (11) leads to

$$\boldsymbol{q} = -\boldsymbol{D}_{11}^{-1} \boldsymbol{D}_{10} \boldsymbol{p} , \tag{13}$$

which is substituted into Eq. (10), results

$$\boldsymbol{v}_0 = \left[\boldsymbol{D}_{00} - \boldsymbol{D}_{01} \boldsymbol{D}_{11}^{-1} \boldsymbol{D}_{10}\right] \boldsymbol{p} = \boldsymbol{F} \boldsymbol{p} . \tag{14}$$

Now, for the stress resultant in a structure, we have

$$\boldsymbol{r} = \left[\boldsymbol{B}_0 - \boldsymbol{B}_1 \boldsymbol{D}_{11}^{-1} \boldsymbol{D}_{10}\right] \boldsymbol{p} . \tag{15}$$

3 Bipartite graph method for selection of a suboptimal general cycle basis

The bipartite graph of a planar truss S, consisting of rectangular panels with or without diagonal members, is constructed as follows.

Associate one with each row of panels and denote them by r_1, r_2, …, r_m. similarly, with each column of panels, associate one node and denote them by c_1, c_2, …, c_n, as illustrated in Fig. 1 (a). Connect r_i to c_j if the corresponding panel in S has a diagonal member as shown in Fig. 1 (b). The graph obtained in this manner is called the bipartite graph $B(S)$ of S. A cycle of $B(S)$ corresponded to a substructure of S that contains a generalized cycle [27]. For localizing the self-equilibrating stress systems, the cycles for which $|c_{max} - c_{min}| + |r_{max} - r_{min}|$ should be chosen [27].

For an irregularity in the boundaries of planar truss, this method can still be used [27]. For this purpose, virtual members can be added in the deficient regions to make the graph completely rectangular. The effect of such members should be included in the process of generating structure's self-equilibrating stress systems. Furthermore, if necessary, the rotation function, as described in Sections 4 and 5, can be applied.

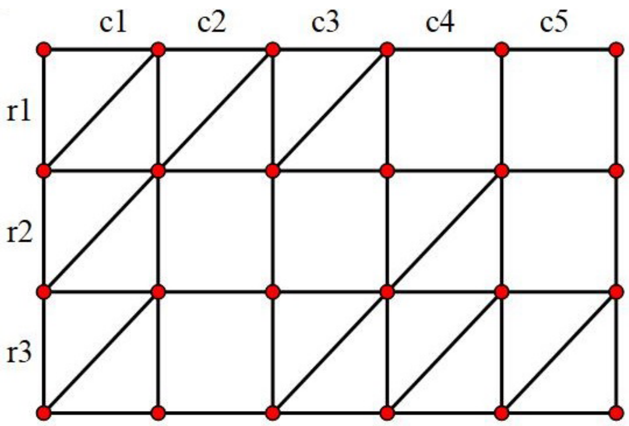

(a)

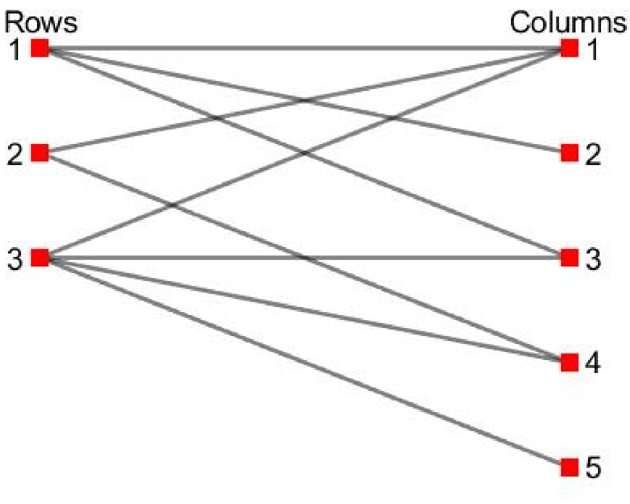

(b)

Fig. 1 (a) A planar truss S and (b) its bipartite graph $B(S)$

4 Rotation function

Kaveh [28], Kaveh et al. [29] and Kaveh and Rahmani [30] have previously been researched on the application of rotation function in the structural analysis. For a two-dimensional graph, the function of rotation, rotates a graph S with respect to a specific node O and a predefined angle Ω.

This function can be stated as follows:

$$S_j = \mathrm{ROT}\left(S_i, O, \Omega\right). \tag{16}$$

Fig. 2 illustrates the rotation function applied to a graph. As shown in Fig. 2, graph S_j that represented by dashed lines, is generated by rotating graph S_i (solid lines) by 90 degrees about the reference node, which is indicated by a cross.

Accordingly, for the structures which do not satisfy the geometric requirements for the bipartite-graph based method to identify the self-equilibrating stress systems, the rotation function would be applied to the simplified equivalent graph model of structure. Fig. 3 presents a flowchart to clarify the steps of the automated procedure and to enhance the reproducibility of the proposed algorithm.

5 Examples

In Section 5, 3 examples are provided to show the efficiency of the proposed procedure.

5.1 Example 1: A 60-bar planar truss

The geometry and external point loads of the 60-bar planar truss are shown in Fig. 4. This structure was previously investigated by Kaveh [23] through the associate graph method. For this truss, DSI = $m - 2n + 3 = 13$.

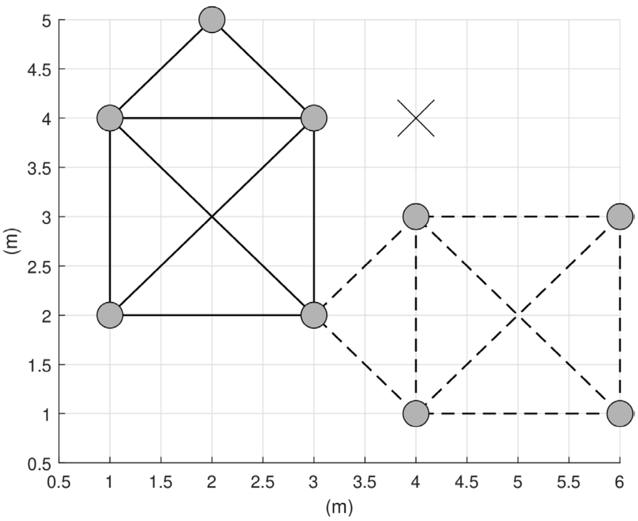

Fig. 2 An example for the rotation function

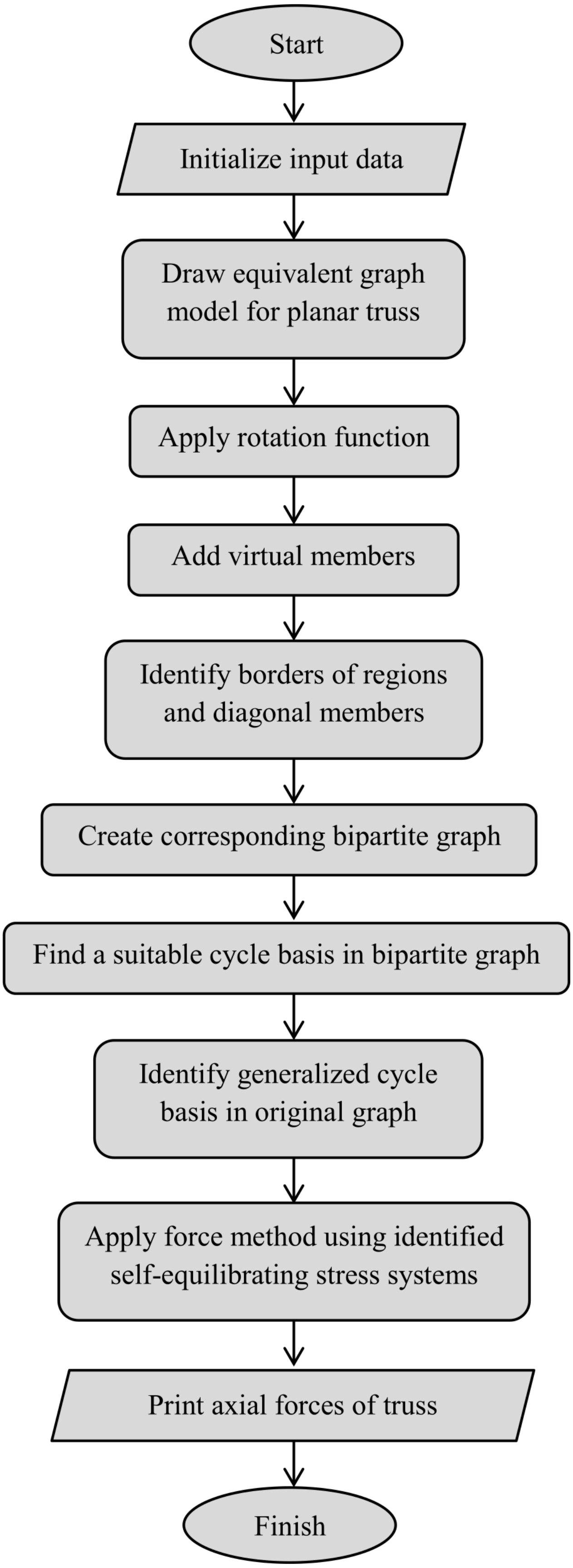

Fig. 3 Schematic flowchart of the proposed automated algorithm

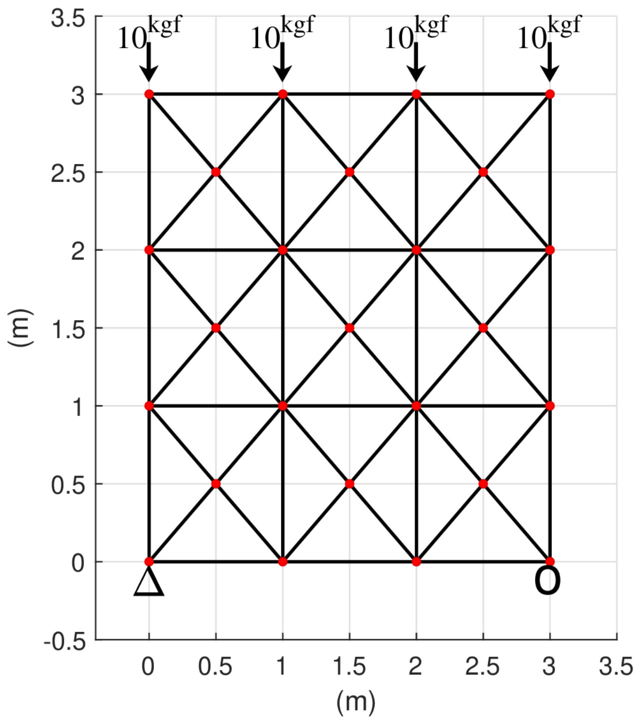

Fig. 4 Geometry, external point loads and support constraints of the 60-bar planar truss

Therefore, the number of generalized cycles for this truss is equal to 13.

Due to the geometry of this structure, it is required to rotate it by 45 degrees around the central node using the rotation function. Additionally, several virtual members — indicated by dashed lines — should be added to the graph as shown in Fig. 5. Furthermore, the corresponding bipartite graph for 60-bar truss is drawn, as shown in Fig. 6.

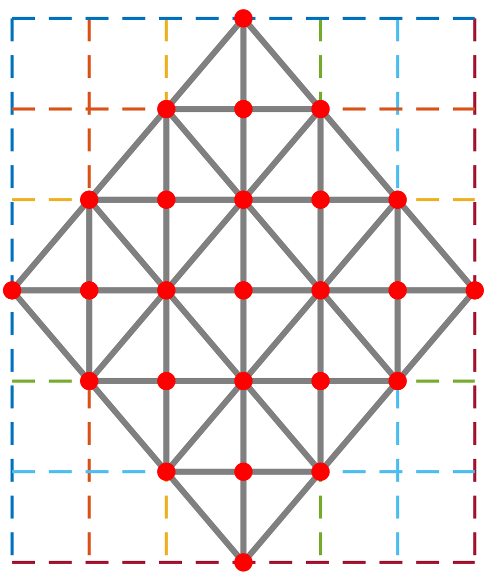

Fig. 5 Rotated graph and virtual members for the 60-bar truss

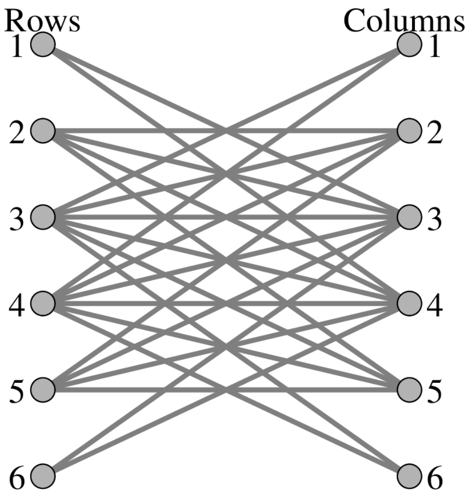

Fig. 6 The corresponding bipartite graph for the 60-bar truss

After the identification of a suitable cycle basis in the above-mentioned bipartite graph, as shown in Fig. 7, the members associated with these cycles in the original graph are selected. The collection of these members forms a generalized cycle in the original structure. Accordingly, the selected generalized cycles for the 60-bar truss are illustrated in Fig. 8.

Fig. 9 depicts the $\boldsymbol{B}_0$ and $\boldsymbol{B}_1$, which are calculated using the self-equilibrated stress systems extracted in the previous step. The pattern of non-zero elements of $\boldsymbol{B}_1 \times \boldsymbol{B}_1^{\mathrm{T}}$ is illustrated in Fig. 10 (a). Subsequently, $\boldsymbol{D}$ is derived using these matrices, as shown in Fig. 10 (b). For a clear comparison, the dimensions of $\boldsymbol{D}_{11}$ which referring as the flexibility matrix of structure, is 13 × 13, while the displacement

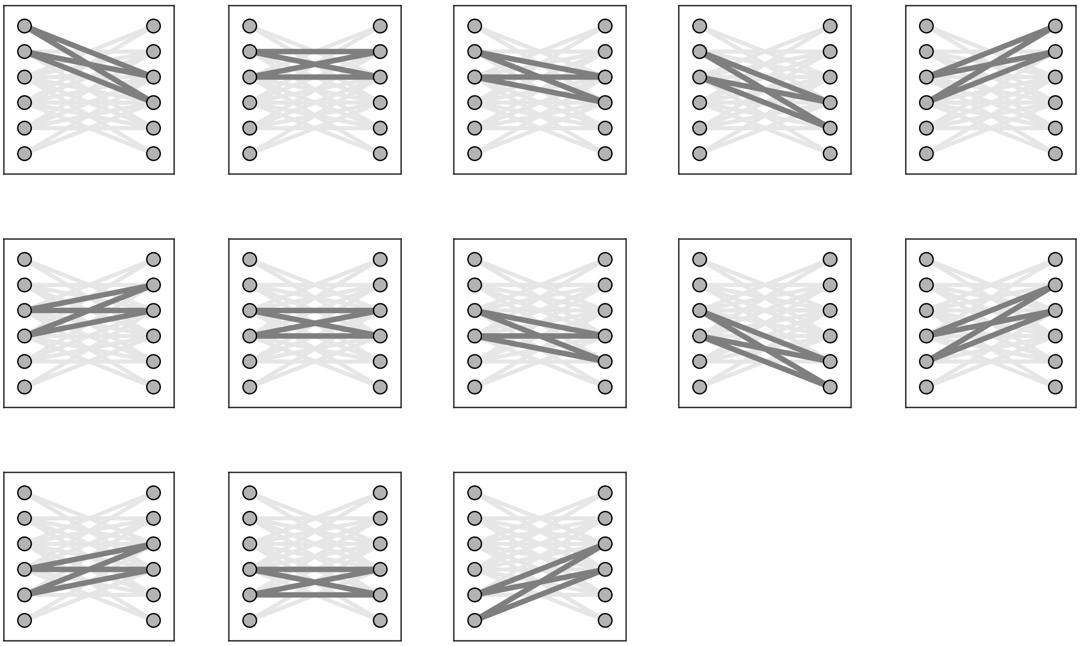

Fig. 7 A suitable cycle basis in the corresponding bipartite graph for the 60-bar truss

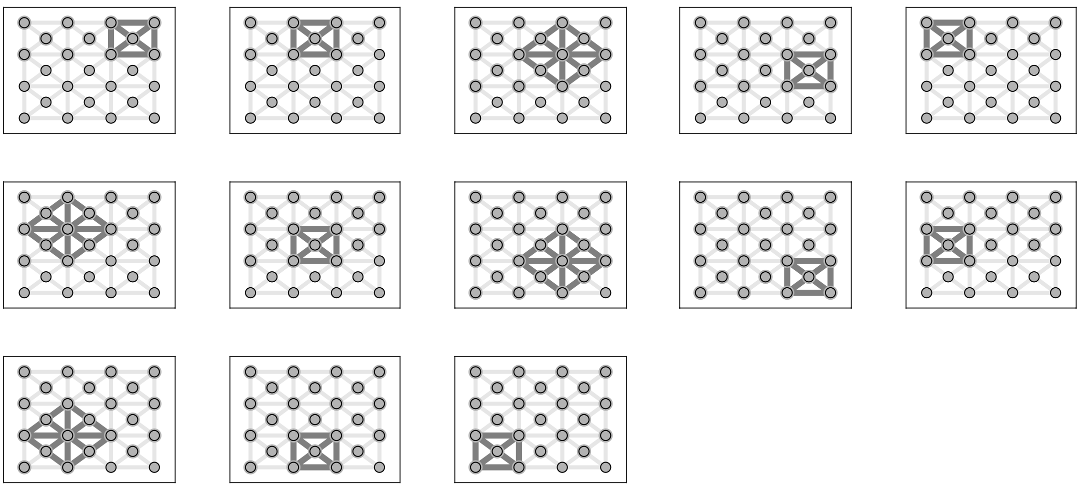

Fig. 8 Extracted generalized cycle basis for the 60-bar truss

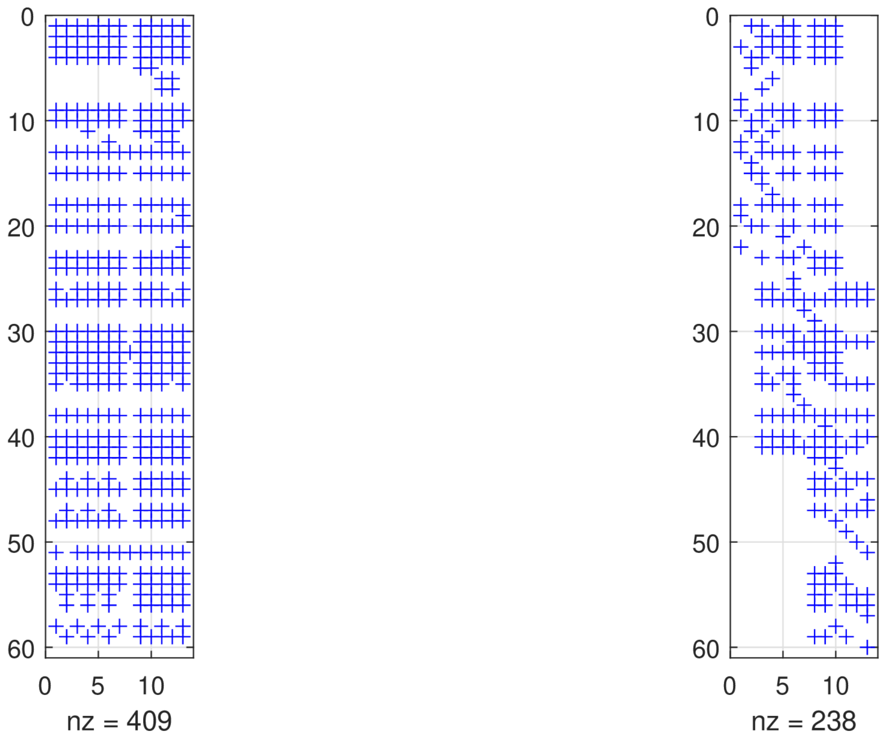

(a) (b)

Fig. 9 (a) Pattern of non-zero elements in $\boldsymbol{B}_0$ and (b) $\boldsymbol{B}_1$ for the 60-bar truss

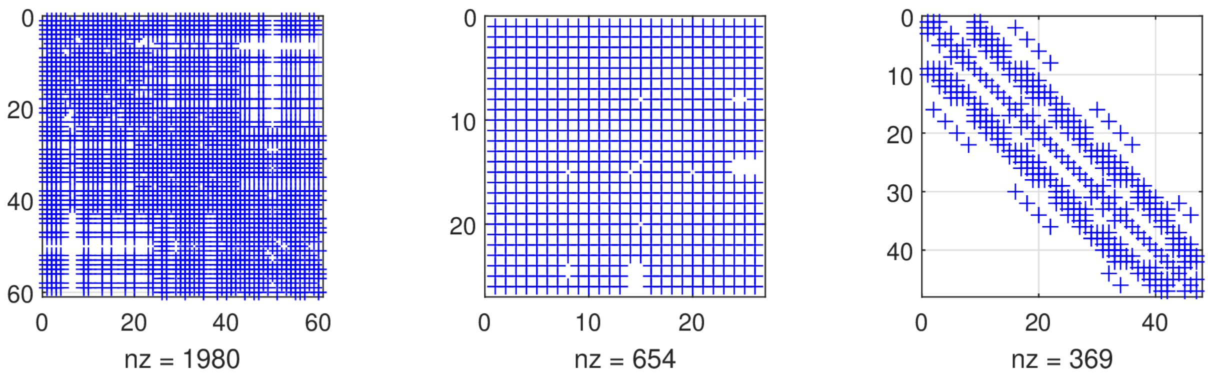

(a) (b) (c)

Fig. 10 (a) Pattern of non-zero elements in $\boldsymbol{B}_1 \times \boldsymbol{B}_1^{\mathrm{T}}$, (b) $\boldsymbol{D}$ and (c) reduced stiffness matrix for the 60-bar truss

method results in a 47 × 47 reduced stiffness matrix, as shown in Fig. 10 (c). This highlights the smaller size of the flexibility matrix, which leads to less storage requirements and computational cost. Finally, the internal forces of 60-bar truss are calculated and illustrated in Fig. 11.

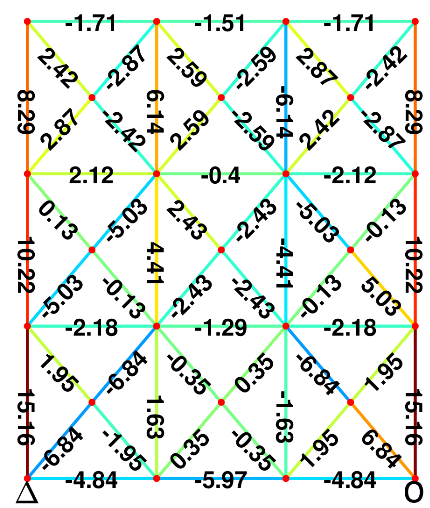

Fig. 11 Axial forces for the 60-bar planar truss (member forces in kgf)

5.2 Example 2: A 153-bar planar truss

The geometry, external loading and support constraints of a 153-bar planar truss shed are illustrated in Fig. 12. This structure was previously investigated by Kaveh and Khavaninzadeh [25] through the associate graph method. In the present study, it is analyzed using the bipartite graph approach using a fully automated procedure, which is implemented in MATLAB [26].

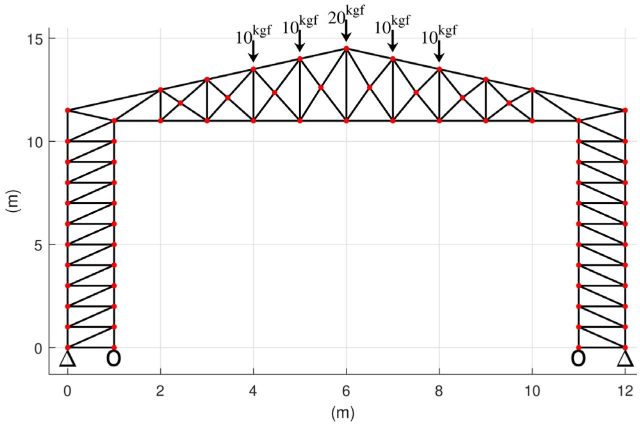

Fig. 12 Geometry, external point loads and support constraints for the 153-bar planar truss

Due to the structural symmetry, only half of the truss is considered for analysis, as shown in Fig. 13. Obviously, since the truss structure, the applied loads, and the support constraints are symmetric before deformation, the structure must remain symmetric after deformation.

In the next step, the graph S is drawn with a simplified geometry. It should then rotated by 45 degrees around one of its nodes using the rotation function. Additionally, in the specified region where the self-equilibrated systems are intended to form, the virtual members are added, as shown in Fig. 14. Based on the rows and columns defined in this specified region, the bipartite graph is constructed as shown in Fig. 15.

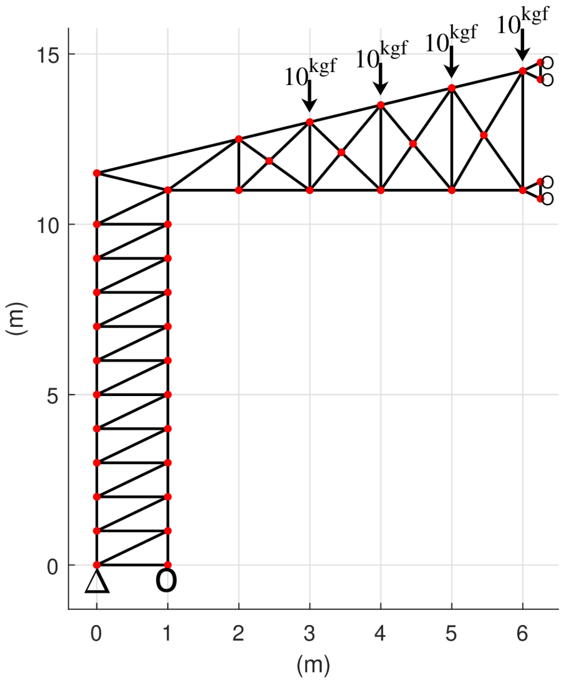

Fig. 13 The half model of the 153-bar truss shed

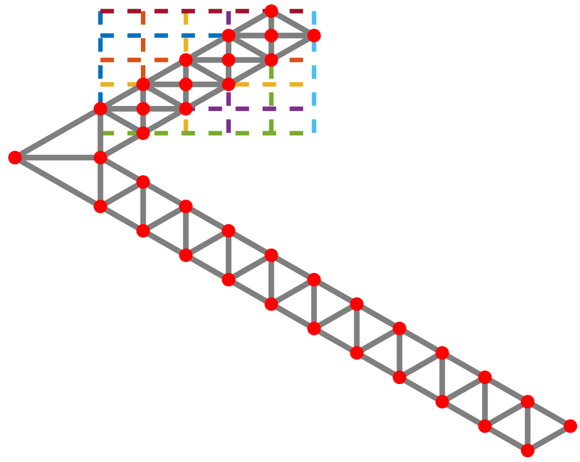

Fig. 14 Rotated graph and additional virtual members for the half model of the 153-bar truss

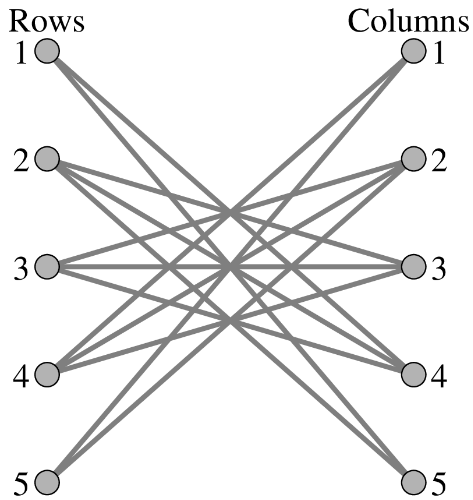

Fig. 15 Corresponding bipartite graph for the half model of the 153-bar truss

To derive the required SESs in the main structure, a maximal set of independent cycles are identified in the bipartite graph, as shown in Fig. 16.

In the next step, the generalized cycles of the structure are identified and illustrated in Fig. 17 using the bipartite graph. The remaining required redundants are selected from the support constraints which were added to the structure due to the symmetry conditions.

Fig. 18 depicts the non-zero elements in $\boldsymbol{B}_0$ and $\boldsymbol{B}_1$. The pattern of non-zero elements in $\boldsymbol{B}_1 \times \boldsymbol{B}_1^{\mathrm{T}}$ is shown in Fig. 19 (a). After computing these matrices, $\boldsymbol{D}$ is derived, as presented in Fig. 19 (b). Accordingly, the dimensions of $\boldsymbol{D}_{11}$, which referring as the flexibility matrix of structure, is 5 × 5, while the displacement method results in a 71 × 71 reduced stiffness matrix, as shown in Fig. 19 (c). This highlights the smaller size of the flexibility matrix,

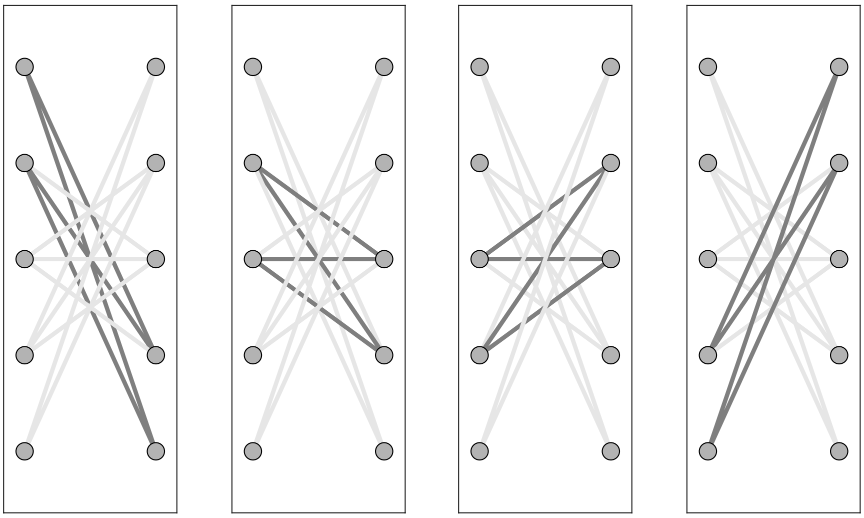

Fig. 16 A cycle basis in the bipartite graph for the half model of the 153-bar truss

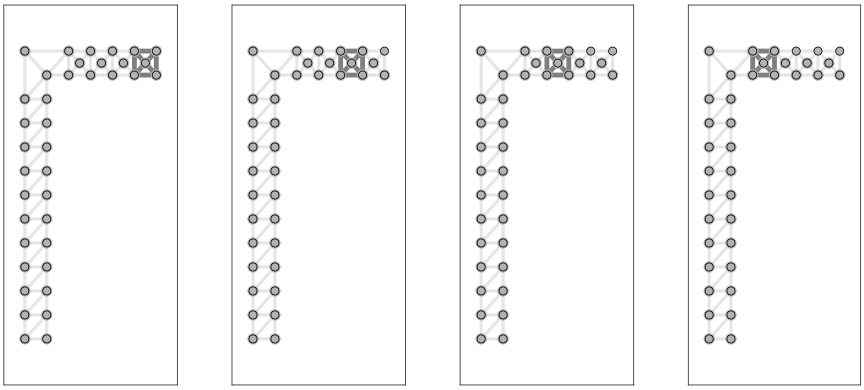

Fig. 17 Extracted generalized cycle basis for the half model of the 153-bar truss

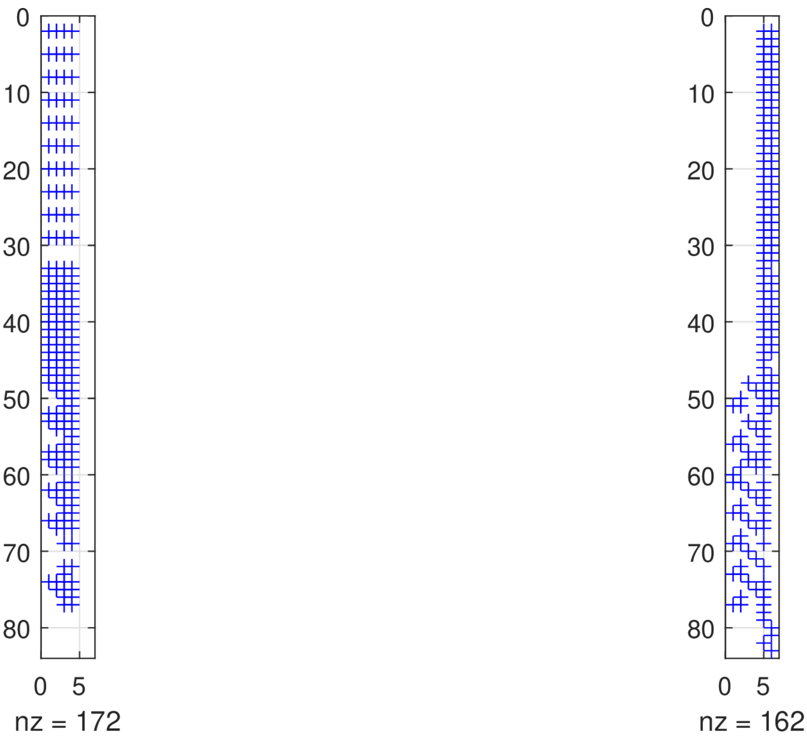

(a) (b)

Fig. 18 (a) Pattern of non-zero elements in $\boldsymbol{B}_0$ and (b) $\boldsymbol{B}_1$ for the half model of the 153-bar truss

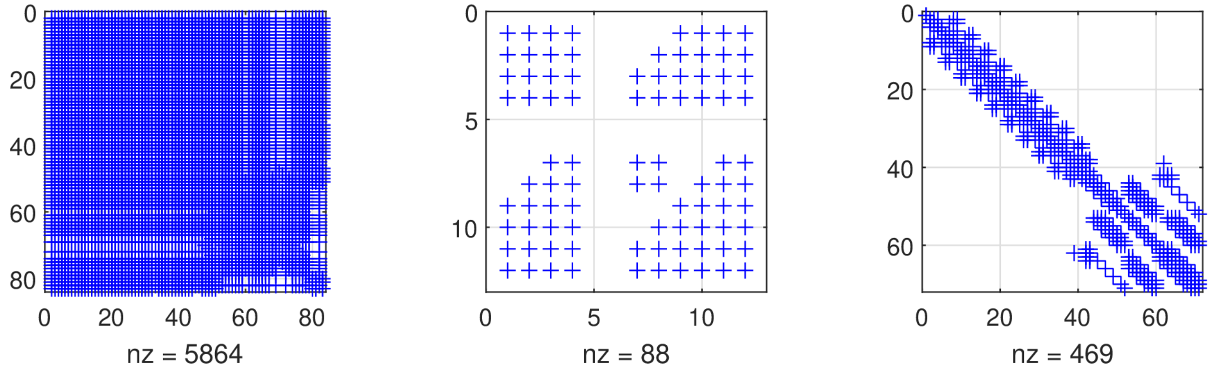

(a) (b) (c)

Fig. 19 (a) Pattern of non-zero elements in $\boldsymbol{B}_1 \times \boldsymbol{B}_1^{\mathrm{T}}$, (b) $\boldsymbol{D}$ and (c) reduced stiffness matrix for the half model of the 153-bar truss

which leads to less storage requirements and computational cost. Finally, the axial forces in the half model of the 153-bar planar truss are calculated as shown in Fig. 20.

5.3 Example 3: A 149-bar planar truss shed

Fig. 21 depicts the geometry and external point loads for a 149-bar truss shed. This truss was previously investigated

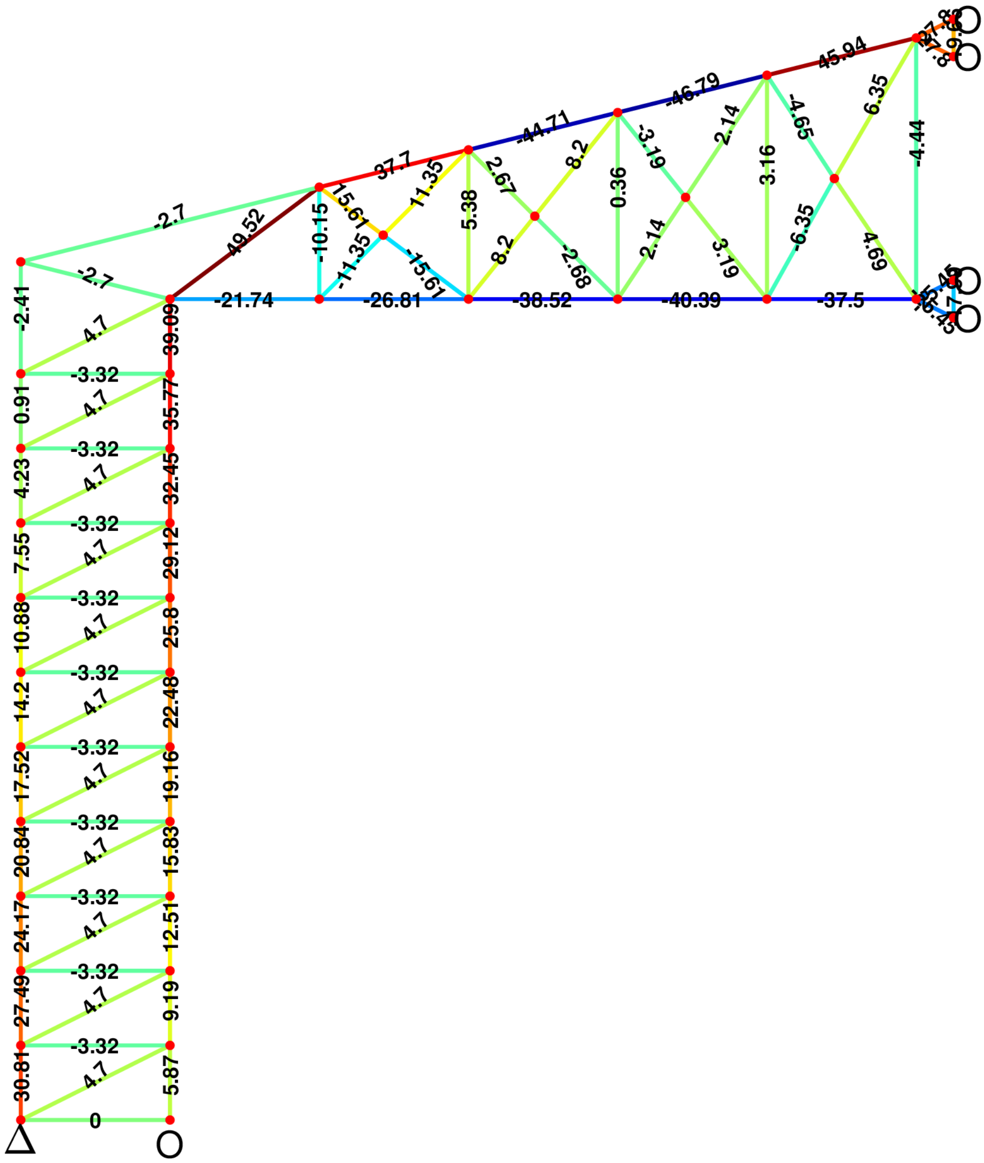

Fig. 20 Axial forces for the half model of the 153-bar truss (kgf)

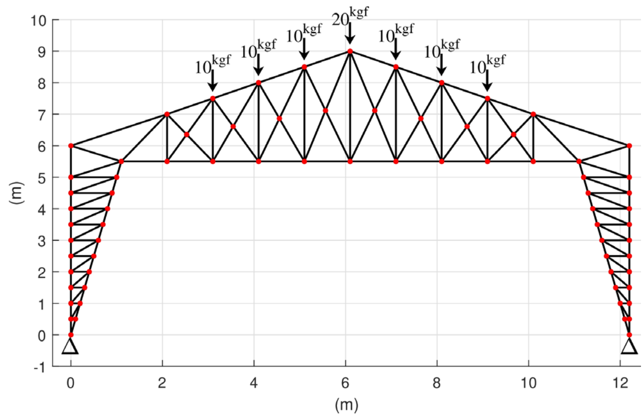

Fig. 21 Geometry, external loading and support constraints for the 149-bar truss shed

by Kaveh and Khavaninzadeh [25] using the associated graph method. In this study, the corresponding bipartite graph is employed to extract the self-equilibrating stress systems. Similar to previous example, due to the symmetry only half of the structure will be analyzed, as shown in Fig. 22.

Due to the geometry of structure, a simplified graph corresponding to the half of the 149-bar planar truss is constructed and rotated by 45 degrees using the rotation function about a reference node. Next, in the specified region where the self-equilibrated systems are intended to form, the virtual members are added, as shown in the Fig. 23. It is important to note that the virtual members participate only in the formation of the bipartite graph.

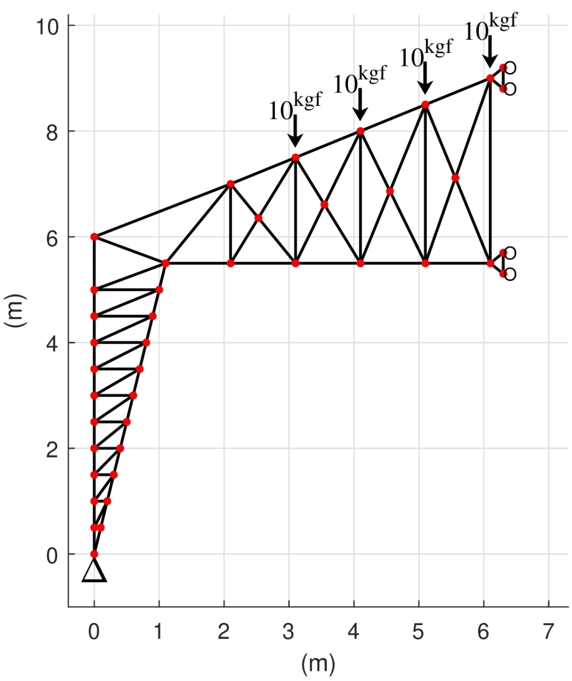

Fig. 22 Geometry, external loading and support constraints for the half model of the 149-bar truss example

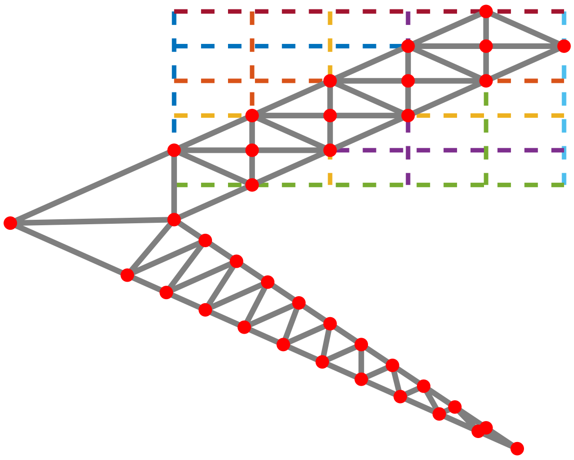

Fig. 23 Rotated graph with its virtual members for the half model of the 149-bar truss

Finally, the bipartite graph corresponding to the specified region is established, as shown in Fig. 24. To derive the required self-equilibrating stress systems in the main structure, a maximal set of independent cycles are identified in the bipartite graph, as shown in Fig. 25.

Fig. 26 presents 4 generalized cycles extracted from the structure within the specified region using the bipartite graph method. The remaining required redundants are selected from the support constraints which were added to the structure due to the symmetry conditions.

Accordingly, $\boldsymbol{B}_0$ and $\boldsymbol{B}_1$ are computed, as shown in the Fig. 27 (a) and (b). Furthermore, the pattern of non-zero elements in the $\boldsymbol{B}_1 \times \boldsymbol{B}_1^{\mathrm{T}}$ is also presented in Fig. 28 (a). Using these matrices, $\boldsymbol{D}$ is subsequently derived as shown in Fig. 28 (b). The dimensions of $\boldsymbol{D}_{11}$, which referring as the flexibility matrix of structure, is 4 × 4, while the displacement method results in a 70 × 70 reduced stiffness matrix, as

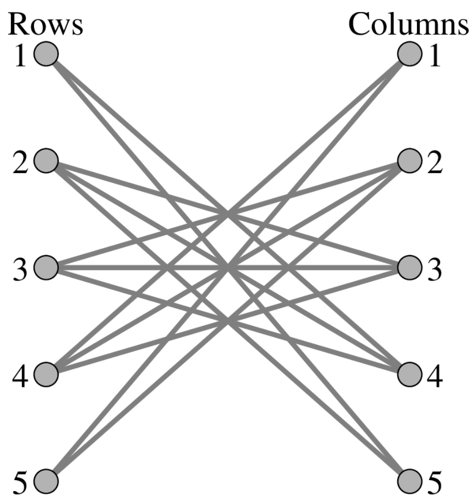

Fig. 24 Corresponding bipartite graph for the half model of the 149-bar truss

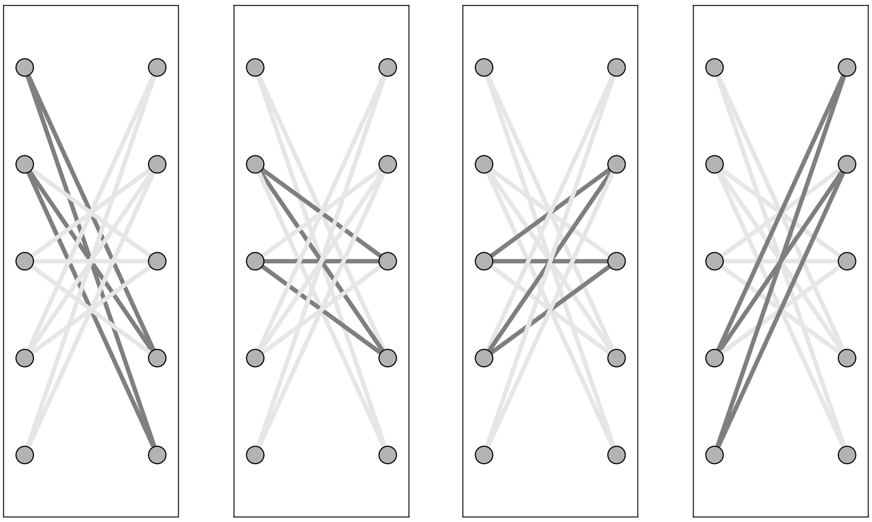

Fig. 25 A cycle basis in the bipartite graph for the half model of the 149-bar truss

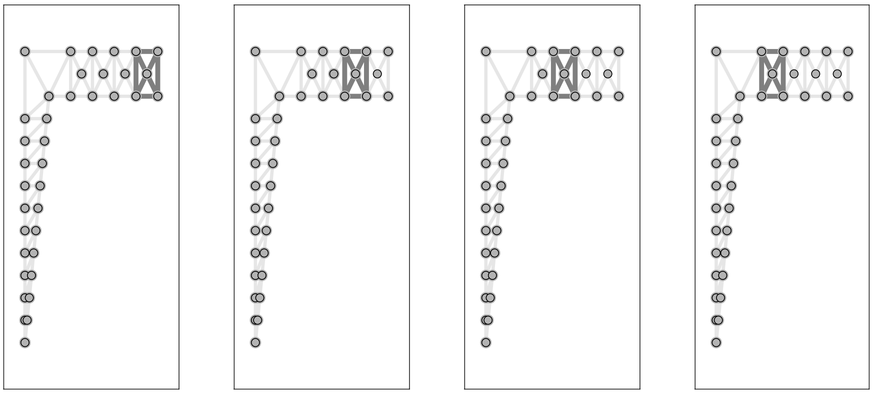

Fig. 26 Extracted generalized cycle basis for the half model of the 149-bar truss

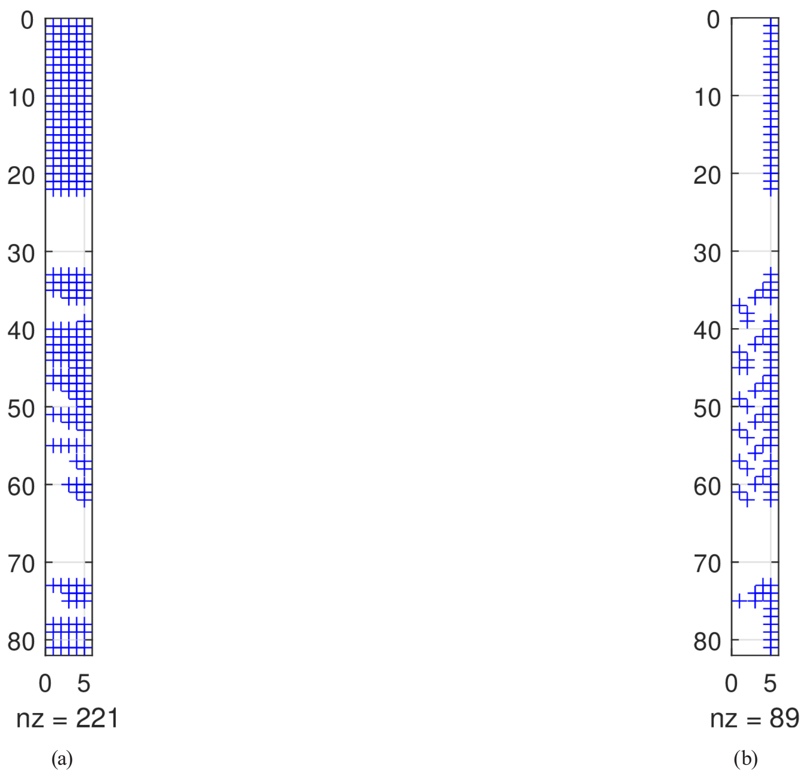

Fig. 27 (a) Pattern of non-zero elements in $\boldsymbol{B}_0$ and (b) $\boldsymbol{B}_1$ for the half model of the 149-bar truss

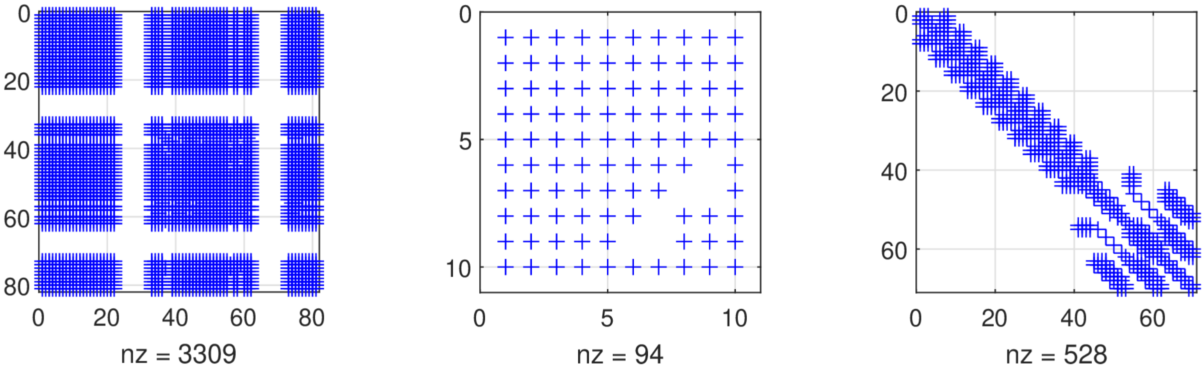

(a) (b) (c)

Fig. 28 (a) Pattern of non-zero elements in $\boldsymbol{B}_1 \times \boldsymbol{B}_1^{\mathrm{T}}$, (b) $\boldsymbol{D}$ and (c) reduced stiffness matrix for the half model of the 149-bar truss

shown in Fig. 28 (c). This highlights the smaller size of the flexibility matrix, which leads to less storage requirements and computational cost. Finally, the internal forces of the structure are determined and illustrated in Fig. 29.

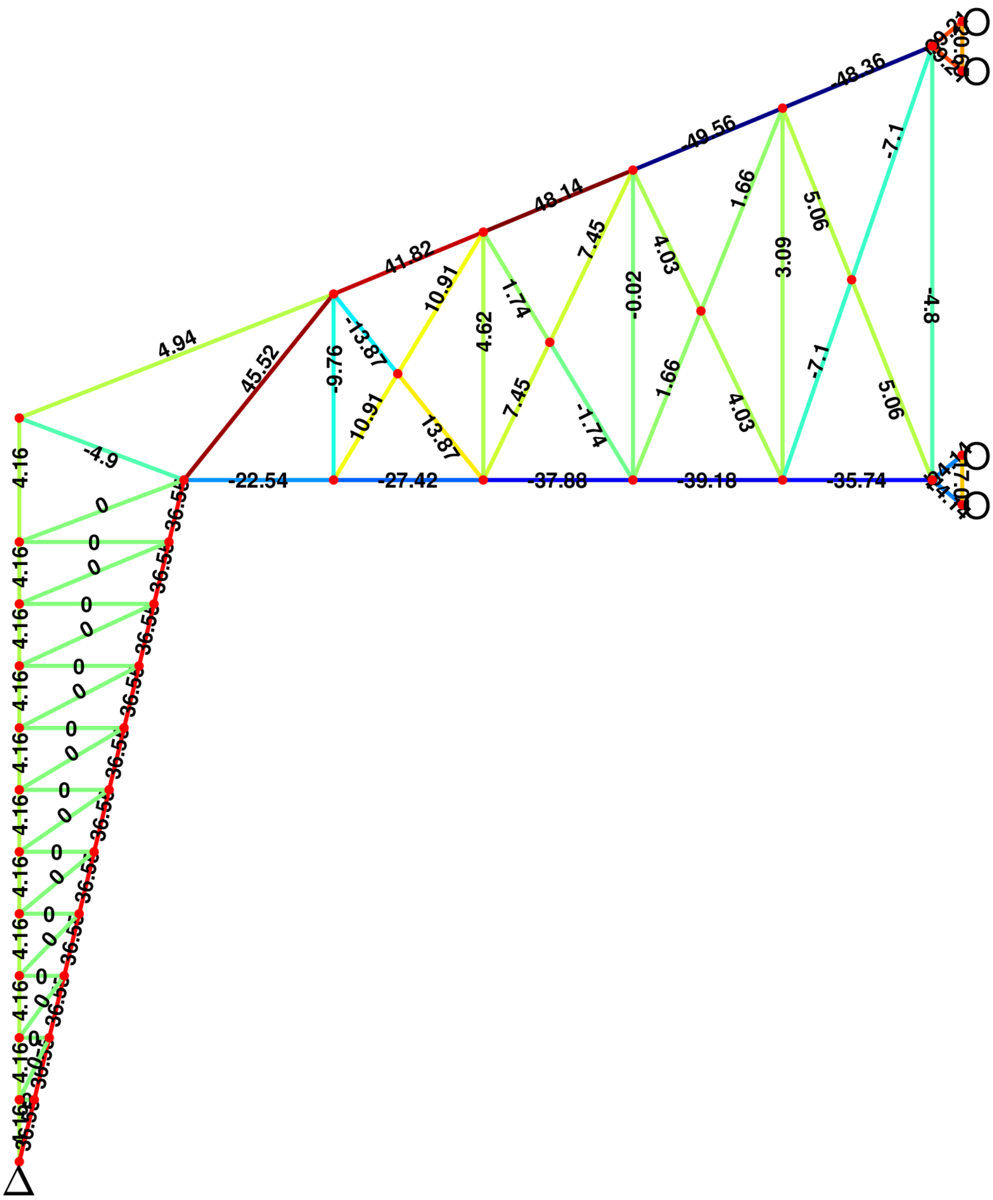

Fig. 29 Axial forces for the half model of the 149-bar truss shed (kgf)

6 Conclusions

In this article, a fully automated procedure for the efficient analysis of truss structures, employing a bipartite graph based force method, was developed and implemented in MATLAB [26]. To extend the applicability of the method, the rotation function and virtual members are automatically applied within this procedure to the planar truss structures that do not satisfy the geometric requirements of this method. Accordingly, after the identification of a suitable cycle basis in the corresponding bipartite graph, which is generated according to the rotated graph including virtual members, the members associated with these cycles are selected in the main structure. The collection of these members forms a self-equilibrating stress system in the truss structure. The resulting matrices obtained from the proposed procedure have a sparse structure, and the results demonstrate the accuracy and efficiency of the performed approach.

References

[1] De C. Henderson, J. C. "Topological Aspects of Structural Linear Analysis: Improving the Conditioning of the Equations of Compatibility of a Multi-Member Skeletal Structure by Use of the Knowledge of Topology", Aircraft Engineering, 32(5), pp. 137–141, 1960. https://doi.org/10.1108/eb033249

[2] De Henderson, J. C. C., Maunder, E. A. W. "A problem in applied topology: on the selection of cycles for the flexibility analysis of skeletal structures", IMA Journal of Applied Mathematics, 5(2), pp. 254–269, 1969. https://doi.org/10.1093/imamat/5.2.254

[3] Kaveh, A. "The application of topology and metroid theory to the analysis of structures", PhD Thesis, University of London, 1974.

[4] Kaveh, A. "Optimal structural analysis", John Wiley & Sons, 2006. ISBN 9780470030158 https://doi.org/10.1002/9780470033326

[5] Kaveh, A. "An efficient program for generating subminimal cycle bases for the flexibility analysis of structures", Communications in Applied Numerical Methods, 2(4), pp. 339–344, 1986. https://doi.org/10.1002/cnm.1630020403

[6] Kaveh, A. "Improved cycle bases for the flexibility analysis of structures", Computer Methods in Applied Mechanics and Engineering, 9(3), pp. 267–272, 1976. https://doi.org/10.1016/0045-7825(76)90031-1

[7] Kaveh, A. "A combinatorial optimization problem; Optimal generalized cycle bases", Computer Methods in Applied Mechanics and Engineering, 20(1), pp. 39–51, 1979. https://doi.org/10.1016/0045-7825(79)90057-4

[8] Denke, P. H. "A general digital computer analysis of statically indeterminate structures", NASA Aeronautics and Space Administration, Washington, DC, USA, Rep. NASA TN D-1666, 1962.

[9] Robinson, J., Haggenmacher, G. W. "Some new developments in matrix force analysis", In: Gallagher, R. H., Yamada, Y., Oden, J. T. (eds.) Recent Advances in Matrix Methods of Structural Analysis and Design, University of Alabama in Huntsville, Huntsville, AL, USA, 1971, pp. 183–228.

[10] Topçu, A. "A contribution to the systematic analysis of finite element structures using the force method", PhD Thesis, University of Essen, 1979.

[11] Kaneko, I., Lawo, M., Thierauf, G. "On computational procedures for the force method", International Journal for Numerical Methods in Engineering, 18(10), pp. 1469–1495, 1982. https://doi.org/10.1002/nme.1620181004

[12] Soyer, E., Topcu, A. "Sparse self-stress matrices for the finite element force method", International Journal for Numerical Methods in Engineering, 50(9), pp. 2175–2194, 2001. https://doi.org/https://doi.org/10.1002/nme.119

[13] Kaveh, A., Shabani Rad, A. "Metaheuristic-based optimal design of truss structures using algebraic force method", Structures, 50, pp. 1951–1964, 2023. https://doi.org/10.1016/j.istruc.2023.02.123

[14] Gilbert, J. R., Heath, M. T. "Computing a sparse basis for the null space", SIAM Journal on Algebraic Discrete Methods, 8(3), pp. 446–459, 1987. https://doi.org/10.1137/0608037

[15] Coleman, T. F., Pothen, A. "The Null Space Problem I. Complexity", SIAM Journal on Algebraic Discrete Methods, 7(4), pp. 527–537, 1986. https://doi.org/10.1137/0607059

[16] Coleman, T. F., Pothen, A. "The Null Space Problem II. Algorithms", SIAM Journal on Algebraic Discrete Methods, 8(4), pp. 544–563, 1987. https://doi.org/10.1137/0608045

[17] Pothen, A. "Sparse null basis computations in structural optimization", Numerische Mathematik, 55(5), pp. 501–519, 1989. https://doi.org/10.1007/BF01398913

[18] Kaveh, A., Rahami, H. "Analysis, design and optimization of structures using force method and genetic algorithm", International Journal for Numerical Methods in Engineering, 65(10), pp. 1570–1584, 2006. https://doi.org/10.1002/nme.1506

[19] Kaveh, A., Bijari, S. "Simultaneous analysis and optimal design of truss structures via displacement method", Scientia Iranica, 27(3), pp. 1176–1186, 2020. https://doi.org/10.24200/sci.2019.51563.2253

[20] Grubits, P., Porrogi, P., Movahedi Rad, M. "Elasto-plastic truss optimization under geometric nonlinearity using a genetic algorithm", Fracture and Structural Integrity, 20(75), pp. 124–156, 2025. https://doi.org/10.3221/IGF-ESIS.75.10

[21] Grubits, P., Movahedi Rad, M. "Automated elasto-plastic design of truss structures based on residual plastic deformations using a geometrical nonlinear optimization framework", Computers & Structures, 316, 107855, 2025. https://doi.org/10.1016/j.compstruc.2025.107855

[22] Kaveh, A. "Statical bases for an efficient flexibility analysis of planar trusses", Journal of Structural Mechanics, 14(4), pp. 475–488, 1986. https://doi.org/10.1080/03601218608907529

[23] Kaveh, A. "Optimal analysis of skeletal structures via force method: a review", International Journal of Optimization in Civil Engineering, 15(3), pp. 359–388, 2025.
https://doi.org/10.22068/ijoce.2025.15.3.644

[24] Kaveh, A., Khavaninzadeh, N. "Optimal design of planar trusses using graph theoretical force method", Periodica Polytechnica Civil Engineering, 67(2), pp. 337–348, 2023.
https://doi.org/10.3311/ppci.21410

[25] Kaveh, A., Khavaninzadeh, N. "Optimization of truss industrial sheds with sloping and arched roofs using the force method and a meta-heuristic algorithm", Scientia Iranica, 2025.
https://doi.org/10.24200/sci.2025.66451.10065

[26] The MathWorks, Inc. "MATLAB, (R2021a)", [computer program] Available at: https://www.mathworks.com/help/releases/R2021a/documentation-center.html

[27] Kaveh, A. "Structural mechanics: graph and matrix methods", Macmillan International Higher Education, 1992. ISBN 1349877603

[28] Kaveh, A. "A graph-theoretical approach to configuration processing", Computers & Structures, 48(2), pp. 357–363, 1993.
https://doi.org/10.1016/0045-7949(93)90428-g

[29] Kaveh, A., Jia, X., Weng, Q. "Rotation as a general operation for configuration processing", Scientia Iranica, 17(2), pp. 131–140, 2010.

[30] Kaveh, A., Rahmani, P. "Canonical forms and rotationally repetitive matrices for eigensolution of symmetric structures", Scientia Iranica, 28(1), pp. 192–208, 2021.
https://doi.org/10.24200/sci.2020.56639.4827